Article

D–π–A–π–D Initiators Based on Benzophenone Conjugate Extension for Two-Photon Polymerization Additive Manufacturing

Shanggeng Li [1,2], **Xiaolin Liu** [3], **Shuai Zhang** [2,*], **Yawen Zhou** [2], **Xiangyu Wan** [2], **Ning Li** [2], **Jing Li** [2] **and Lin Zhang** [2]

1   School of Nuclear Science and Technology, University of Science and Technology of China,
    Hefei 230026, China; lsglsg@mail.ustc.edu.cn
2   Research Center of Laser Fusion, China Academy of Engineering Physics, Mianyang 621900, China;
    zhouyawen163@163.com (Y.Z.); wanxiangyu_caep@126.com (X.W.); lncaep@163.com (N.L.);
    jingli0218@163.com (J.L.); zhlmy@sina.com (L.Z.)
3   School of Physics, University of Science and Technology of China, Hefei 230026, China;
    lxl91003@mail.ustc.edu.cn
*   Correspondence: zhangshuai_scu@126.com; Tel.: +86-0816-2493148

Abstract: A two-photon polymerization initiator is a kind of nonlinear optical material. With the demand for more efficient initiators in two-photon polymerization additive manufacturing, there are more and more related studies. In this paper, four conjugate-extended two-photon polymerization initiators with different alkane chain lengths were designed and synthesized, and single-photon, two-photon, and photodegradation experiments were carried out. Additive manufacturing experiments illustrated that the designed molecules can be used as two-photon initiators, and the writing speed can achieve 100,000 μm/s at a laser power of 25 mW. Through theoretical calculation and experimental comparison of the properties of molecules with different conjugation degrees, it was proven that a certain degree of conjugation extension can improve the initiation ability of molecules; however, this improvement cannot be extended infinitely. Solubility tests of different acrylates showed that molecules with different alkane chain lengths have varying solubility. Changing the molecular alkane chain length may be favorable to adapt to different monomers.

Keywords: optical functional materials; photoinitiator; two-photon polymerization additive manufacturing; conjugation extension; solubility

1. Introduction

Two-photon absorption is a third-order nonlinear optical effect that has a wide range of uses. Among them, two-photon polymerization additive manufacturing (TPPAM) is extensively used in many three-dimensional precision structure manufacturing fields—such as those of photonic crystals [1,2], micro-optical elements [3,4], three-dimensional high-density information storage [5–7], biocompatible devices [8–10], etc.—due to its unique ultra-high-resolution performance. TPPAM has a growing number of applicaitons, which also highlights the new requirements for its manufacturing speed. Since TPPAM is a manufacturing method in which dots form lines and lines form surfaces, making larger structures takes a lot of time to manufacture. Meanwhile, the speed of writing in manufacturing is extremely significant. A larger writing speed can improve manufacturing efficiency and save time.

However, if the writing speed is too high, the resin cannot be irradiated with sufficient laser energy and polymerized to form a three-dimensional structure. One way to solve this problem is to increase the power of the laser. Nevertheless, laser power that is too high will impose high requirements on the laser and increase production costs. Another way is to raise the efficiency of the two-photon polymerization initiator (TPPI). As an important nonlinear material, TPPI absorbs laser energy, undergoes two-photon absorption, generates free radicals, and initiates polymerization [11]. Therefore, it only requires a more efficient

initiator if the speed of writing in manufacturing is to be faster, which can lead to the absorbtion of more photons or the production of more free radicals.

As a consequence, the key to the solving this problem is to improve the efficiency of the initiator. In the early days, TPPI used conventional ultraviolet (UV) photoinitiators. UV photoinitiators have active groups and generate free radicals under ultraviolet light irradiation. However, the absorption band of ultraviolet photoinitiators is mainly located in the ultraviolet region, and the two-photon absorption cross section (δ_{TPA}) is also small. The possibility of two-photon absorption is so low that the low initiation efficiency is rendered. Studies have proven that by performing conjugation extension, the δ_{TPA} of the molecule can be effectively increased, and the absorption efficiency of light can be raised, thereby improving the efficiency of the initiator [12–14]. Conjugation extension is the introduction of conjugated groups to connect electron acceptors and electron donors, as well as increase the degree of molecular conjugation and intramolecular charge transfer (ICT) [15–17]. Currently, the efficiency of initiators through conjugation expansion has been improved in many studies [18–25]. These studies concluded that molecules make up the structures donor–π–acceptor (D–π–A), donor–π–acceptor–π–donor (D–π–A–π–D), acceptor–π–donor–π–acceptor (A–π–D–π–A), etc., would have better ICT and, thus, have larger δ_{TPA} and initiator efficients. However, it is clear that there is a limit to the enhancement of molecular initiation properties through conjugation extension. It is interesting to question, then, where the performance limits can be improved using this approach.

In addition, the compatibility of molecules and monomers is also essential. The initiator molecule must be completely dissolved in the monomer to be effective. Often monomers with different types of structures have different requirements for initiator molecules. For example, the initiators used to print hydrogels need to be water-soluble [26,27]. However, it is very difficult under the condition that one kind of initiator can be widely used in various polar resins. For each monomer, molecular design considering solubility is extremely complicated, and it is not conducive to practical production applications. Therefore, it would be interesting if there was a way to change the structure of the molecule in small amounts, effectively improving the solubility of the molecule with different monomers. The alkane chain is a very easily overlooked part because it hardly affects the chemical properties of the molecule. However, the length of the alkane chain will affect the polarity, the degree of steric hindrance and the geometric configuration of the molecule, and thus, the solubility of the molecule. Moreover, due to the alkane chain hardly affecting the chemical properties of the molecule, changing the length of the alkane chain hardly affects the synthesis method and manufacturing process of the molecule, which greatly reduces the cost of practical application.

In view of the above two points, the traditional UV photoinitiator BD-PM with an active structure was conjugated and extended by introducing a benzene ring to obtain the molecules BD-PPM and BM-PPPM, as shown in Figure 1. Among them, BD-PPM molecules have been reported in the literature with similar structures, and certain effects have been achieved [28]. BM-PPPM with two benzene rings has a larger degree of conjugation. In the previous work, the molecules (BM-PTM) with a larger degree of conjugation formed by benzophenone and triphenylamine were studied, and also obtained good results [29]. New groups can be introduced because diphenylamine has one more site on the nitrogen atom than triphenylamine. Hence, the alkane chain will affect the solubility of the molecule, and the length of the alkane chain on the diphenylamine is simply changed for the molecule BM-PPPM, so that initiators suitable for various monomers can be obtained. This paper compares the initiation properties of molecules with different degrees of conjugation and investigated whether BM-PPPM series molecules can be better considered as initiators.
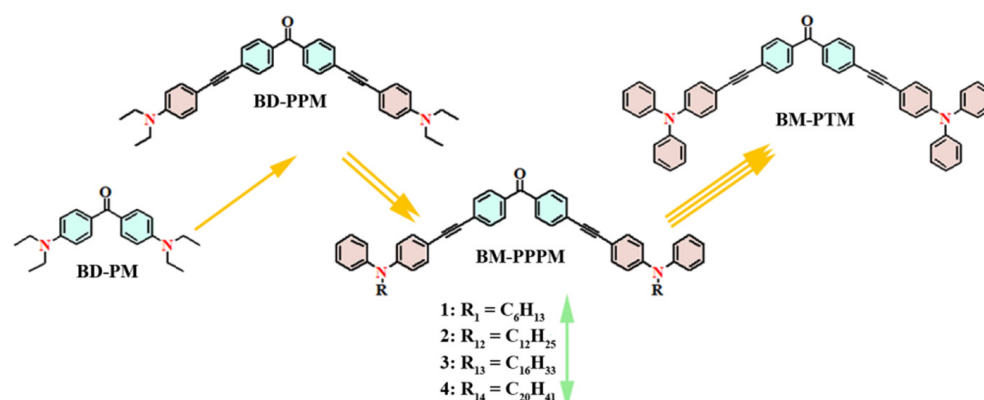
Figure 1. The structural formulas of BD-PM (UV photoinitiator), BD-PPM [28], BM-PPPM and BM-PTM [29].

2. Theory Calculation

The DFT approach can be used to calculate the frontier orbits of conjugated molecules such as D–π–A–π–D and A–π–D–π–A, and to observe the degree of intramolecular charge transfer, so as to predict the two-photon absorption characteristics of the molecule [30,31]. To probe into the electronic properties of molecules with different conjugation extension degrees, the theoretical calculations were carried out using the DFT approach, and the B3LYP functional and 6-31G(d, p) basis sets were used with Gaussian 09 [32]. For molecules with three different degrees of conjugation extension, the degree of intramolecular charge transfer and the frontier orbital energy were analyzed. To reduce the workload of calculations, all alkyl groups were substituted with methyl groups.

It can be seen from Figure 2 that the HOMO orbital was mainly concentrated in the amino part of the electron donor and extended to the π bond bridge, while the LUMO orbital mainly extended from the acetylene bridge to the electron acceptor group benzophenone. With the increases in the conjugation degree, when the BD-PM conjugation was extended to BD-PPM, the ICT of the molecule increased significantly. When extending from BD-PPM to BM-PPPM, the HOMO orbital charge of the molecule was distributed to a further position, along with the introduced conjugated benzene ring, but the LUMO orbital did not change significantly. This probably indicates that the expansion of the electron donor mainly affects the electron distribution of molecules on the HOMO orbital. Overall, the designed molecule BM-PPPM had good ICT performance, which provides a theoretical basis for its application as a TPPAM photoinitiator.
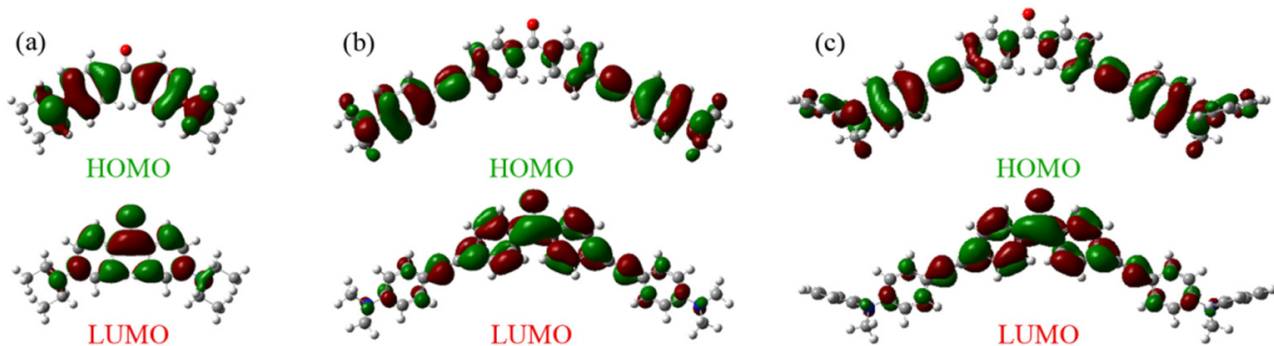
Figure 2. Frontier orbital diagrams of molecules with different degrees of conjugation. HOMO: Highest Occupied Molecular Orbital; LUMO: Lowest Unoccupied Molecular Orbital. (**a**) BD-PM; (**b**) BD-PPM; (**c**) BM-PPPM.

The calculated results of the molecular frontier orbital energy of BD-PM were very close to the known reports [33], which proves the rationality of the calculation. While

the use of the B3LYP functional is suitable for calculations of molecular energies, it also over-planarizes the molecule, and over-delocalizes the wave function. As shown in Table 1, the HOMO energy level of the molecule was significantly increased, the LUMO energy level was significantly decreased, and the band gap was significantly reduced as the BD-PM conjugation was extended to BD-PPM. When BD-PPM was extended to BM-PPPM, the change degree of molecular energy level was reduced significantlyand the band gap was slightly reduced, which is consistent with the result directly observed in Figure 2. This shows that, theoretically, the conjugation of molecules is relatively limited, and it means that the conjugation of the molecule cannot be increased indefinitely by blindly adding conjugated groups.

Table 1. Molecular frontier orbital energy.

	HOMO (eV)	LUMO (eV)	Gap (eV)	Dippole (Debye)
BM-PPPM	−5.01	−1.85	3.16	6.4644
BD-PPM	−4.96	−1.78	3.18	6.5658
BD-PM	−5.71	−1.49	4.21	4.2349

3. Experimental Section

3.1. Materials

All reagents were obtained from commercial suppliers (Table S1) and used without further purification.

3.2. Physical Measurements

Nuclear magnetic resonance (NMR) spectra were obtained on a BRUKER AVANCE III HD 400 MHz (^{1}H NMR at 400 MHz, ^{13}C NMR at 100 MHz). The ^{1}H NMR chemical shifts were measured relative to CDCl$_3$ (δ = 7.26 ppm) as the internal reference. The ^{13}C NMR chemical shifts were given using CDCl$_3$ (δ = 77.16 ppm) as the internal standard. High-resolution mass spectra (HRMS) were obtained with a Thermo Scientific Q Exactive. Absorption spectra were obtained on a HITACHI U-2910 spectrometer. Fluorescence spectra were collected on a Horiba Fluorolog-3 fluorescence spectrometer. The two-photo fluorescence spectra were obtained with MAITAIHP, spectrum physic maitai, and SD2000. The fluorescence quantum yields were measured using a Hamamatsu C11347-11. The cyclic voltammetry tests were performed on an electrochemical workstation (instrument model: CHI660E). Scanning electron microscopes (SEM) were obtained using a Merlin VP Compact, Carl Zeiss.

3.3. Synthesis

Detailed synthetic methods are provided in the Supplementary Materials (Supporting Information) (Figures S1–S3). The synthesis of the final products BM-PPPM was achieved using the classical Sonogashira reaction [34].

BM-PPPM-C6: Purification by column chromatography on silica gel (petroleum ether/ethyl acetate = 10/1, *v/v*) rendered BM-PPPM-C6 as a yellow solid. ^{1}H NMR (400 MHz, CDCl$_3$): δ = 0.88 (t, *J* = 6.8 Hz, 6H), 1.25–1.35 (m, 12H), 1.62–1.72 (m, 4H), 3.70 (t, *J* = 6.8 Hz, 4H), 3.85 (t, *J* = 7.2 Hz, 4H), 6.75–6.79 (m, 4H), 7.11–7.19 (m, 6H), 7.34–7.40 (m, 8H), 7.56–7.62 (m, 4H), 7.74–7.79 (m, 4H) ppm. ^{13}C NMR (CDCl$_3$, 100 MHz): δ = 14.2, 22.8, 26.9, 27.5, 31.8, 52.5, 87.5, 94.1, 111.8, 116.1, 124.5, 125.5, 128.6, 129.8, 130.1, 131.2, 133.0, 136.2, 147.0, 148.8, 195.4 ppm.

BM-PPPM-C12: Purification by column chromatography on silica gel (petroleum ether/ethyl acetate = 15/1, *v/v*) rendered BM-PPPM-C12 as a yellow solid. ^{1}H NMR (400 MHz, CDCl$_3$): δ = 0.88 (t, *J* = 7.2 Hz, 6H), 1.21–1.33 (m, 36H), 1.62–1.72 (m, 4H), 3.70 (t, *J* = 8.0 Hz, 4H), 3.85 (t, *J* = 7.2 Hz, 4H), 6.77 (d, *J* = 8.8 Hz, 4H), 7.12–7.19 (m, 6H), 7.37 (t, *J* = 6.8 Hz, 8H), 7.59 (d, *J* = 8.4 Hz, 4H), 7.77 (d, *J* = 8.4 Hz, 4H) ppm. ^{13}C NMR (CDCl$_3$,

100 MHz): δ = 14.3, 22.9, 27.2, 27.5, 29.5, 29.6, 29.72, 29.76, 29.77, 29.78, 32.1, 52.5, 87.5, 94.1, 111.7, 116.1, 124.4, 125.5, 128.6, 129.8, 130.1, 131.2, 133.0, 136.1, 147.0, 148.8, 195.4 ppm.

BM-PPPM-C16: Purification by column chromatography on silica gel (petroleum ether/ethyl acetate = 15/1, *v/v*) rendered BM-PPPM-C16 as a yellow oil. ^{1}H NMR (400 MHz, CDCl$_3$): δ = 0.84–0.92 (m, 14H), 1.16–1.28 (m, 46H), 1.77–1.86 (m, 2H), 3.63 (d, *J* = 7.2 Hz, 4H), 6.78–6.84 (m, 4H), 7.09–7.18 (m, 6H), 7.32–7.40 (m, 6H), 7.56–7.62 (m, 4H), 7.75–7.79 (m, 4H) ppm. ^{13}C NMR (CDCl$_3$, 100 MHz): δ = 14.25, 14.28, 22.79, 22.83, 26.46, 26.47, 29.5, 29.7, 29.8, 30.2, 31.66, 31.68, 31.95, 32.0, 36.4, 56.9, 87.6, 94.0, 112.1, 116.9, 124.1, 125.3, 128.6, 129.7, 130.1, 131.2, 132.8, 136.2, 147.6, 149.7, 195.4 ppm.

BM-PPPM-C20: Purification by column chromatography on silica gel (petroleum ether/ethyl acetate = 20/1, *v/v*) rendered BM-PPPM-C20 as a yellow oil. ^{1}H NMR (400 MHz, CDCl$_3$): δ = 0.88 (t, *J* = 7.2 Hz, 14H), 1.17–1.28 (m, 62H), 1.75–1.85 (m, 2H), 3.70 (d, *J* = 7.2 Hz, 4H), 6.81 (d, *J* = 8.8 m, 4H), 7.09–7.18 (m, 6H), 7.31–7.40 (m, 6H), 7.56–7.62 (m, 4H), 7.75–7.79 (m, 4H) ppm. ^{13}C NMR (CDCl$_3$, 100 MHz): δ = 14.3, 22.83, 22.85, 26.5, 29.46, 29.51, 29.69, 29.73, 29.78, 29.79, 30.17, 31.67, 32.03, 32.07, 36.34, 56.9, 87.6, 94.0, 112.1, 116.9, 124.1, 125.3, 128.6, 129.7, 130.1, 131.2, 132.9, 136.2, 147.6, 149.7 ppm.

3.4. Resin Preparation

To consider the initiation efficiency and solubility of the initiator under different monomers, two monomers—trimethylolpropane triacrylate (TMPTA) and pentaerythritol triacrylate (PETA)—were adopted. They all had three functional groups, which could achieve a high degree of polymerization and avoid the performance differences caused by different functionalities. Photoresist was prepared by mixing TMPTA, PETA, and 4 kinds of initiator molecules with different chain lengths with BM-PPPM (10 μmol/g), then stirred overnight at 45 °C until clear and free of precipitation. Finally, the mixture was placed in a greenhouse for 24 h to ensure that it did not settle.

3.5. TPPAM Test

The TPPAM experiments were carried out by Nanoscribe GT Photonic Professional, in which the repetition rate was 80 MHz and the wavelength was 780 ± 10 nm. The pulse duration was approximately 120 fs. The average power of laser irradiation on the sample plane was about 50 mW. In the experiment, a 63× objective lens (Numerical aperture 1.4, working distance 190 μm) was adopted. Meanwhile, a three-dimensional wooden-stick stack structure was designed in the experiment under different laser powers and writing speeds, which aimed to test the molecular initiation efficiency and the manufacturing parameter interval for forming a complete three-dimensional structure.

The preparation process adopted an oil-immersion objective lens. After production, the final structure was obtained by being developed twice for 10 min in propylene glycol monomethyl ether acetate (PGMEA), then washed with isopropanol and eventually dried at 40 °C.

4. Results and Discussions

4.1. Linear Absorption and Fluorescence Spectra

As shown in Figure 3, the ultraviolet absorption and fluorescence spectra of molecules BM-PPPM-C6 and BM-PPPM-C12 are, of course, very close. Owing to its chain length, alkane has little effect on the chemical properties of the molecule, only the properties of BM-PPPM-C6 need to be tested. It can be seen from the absorption spectrum that the molecule has a large ultraviolet absorption peak and molar extinction coefficient near 390 nm. This means that molecules have a great utilization of light near this wavelength. It can be speculated that when two-photon absorption occurs, there will be a greater absorption rate for the 780 nm laser.

As can be seen from the fluorescence spectrum of the molecule, the emission wavelength of the fluorescence ehxibits a significant red shift with the increase in the polarity of

the solvent, which indicates that the excitation of molecules has an obvious ICT process. This is conducive to the nonlinear properties of the molecule.
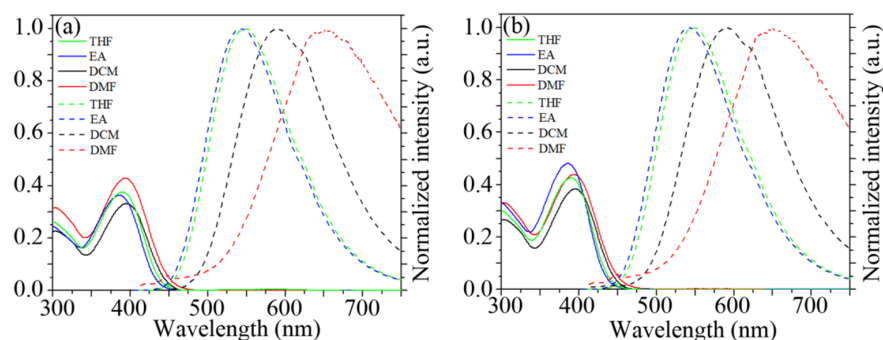
Figure 3. Linear absorption and fluorescence spectra of molecules (**a**) BM-PPPM-C6 and (**b**) BM-PPPM-C12 at a concentration of 1×10^{-5} mol/L and cuvette a cuvette width of 1 cm. THF—tetrahydrofuran; EA—ethyl acetate; DCM—dichloromethane; DMF—N,N-dimethylformamide.

4.2. Two-Photon Fluorescence Spectra

Two-photon fluorescence spectra can reflect the ability of the molecule to undergo two-photon absorption. As the probability of two-photon absorption is proportional to the square of the laser power, according to the relationship between the integral area of the two-photon fluorescence and the laser power at different powers, whether or not the molecule has two-photon absorption can be verified. The fluorescence spectrum is shown in Figure 4a, and the relationship between its integral area and laser power is shown in Figure 4b. As can be seen from the fitted line of the logarithmic relationship, its slope is around 2 and slightly smaller than 2, indicating that two-photon absorption occupies the main part of the molecular excitation mode; this also confirms that the molecule can, indeed, undergo two-photon absorption.
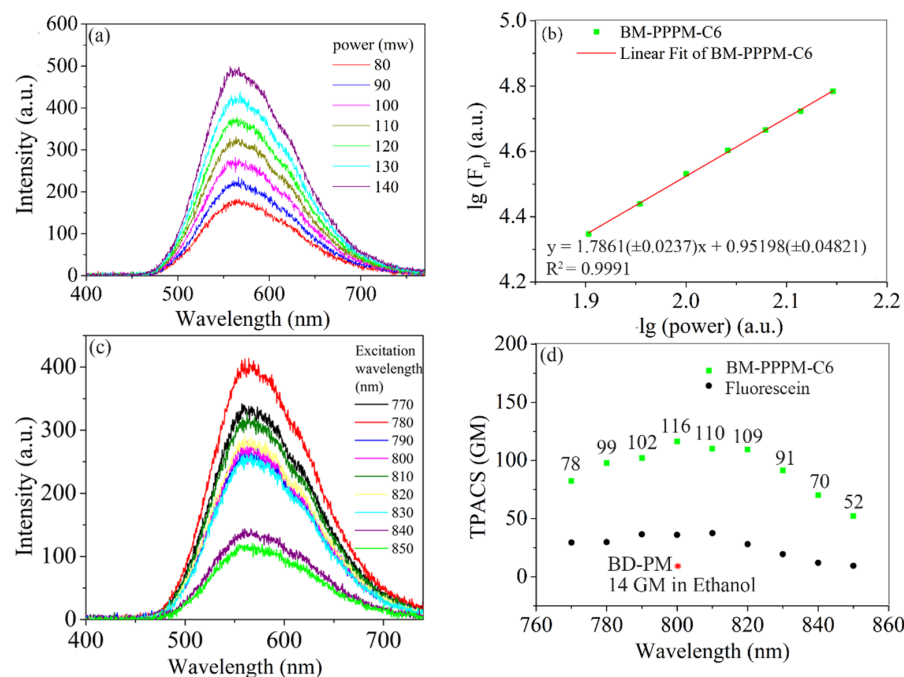

Figure 4. (**a**) Two-photon fluorescence of molecule BM-PPPM-C6 under diverse laser powers at 800 nm in DCM; (**b**) relationship between two-photon fluorescence integration area (F_n) and laser power (mW) of BM-PPPM-C6; (**c**) two-photon fluorescence of molecule BM-PPPM-C6 at diverse excitation wavelengths in DCM; (**d**) TPACS: δ_{TPA} (1 GM = 10^{-50} cm$^4\cdot$s/photon) at diverse wavelengths of molecule BM-PPPM-C6 in DCM.

The intensity of two-photon fluorescence at different wavelengths is shown in Figure 4c. The fluorescence quantum yield of BM-PPPM-C6 was 52.1% in DCM. (Figure S4). Combined with the fluorescence quantum yield data, δ_{TPA} can be calculated using the upconversion fluorescence method [35], as shown in Figure 4d. The fluorescence intensity is distinct at different wavelengths, and the calculated two-photon absorption cross section also varies. It can be seen that the molecule obtains a larger two-photon absorption cross section near 800 nm. It makes certain that the molecule has a greater probability of two-photon absorption, which is a prerequisite to being a two-photon initiator.

At a wavelength of 800 nm, compared with the molecular BD-PM, the δ_{TPA} of BM-PPPM-C6 was 116 GM, while the δ_{TPA} of BD-PM was 14 GM [36]. Therefore, the δ_{TPA} of the molecule was greatly increased. However, the δ_{TPA} of BD-PPM was 336 GM in THF [28], and the δ_{TPA} of BD-PTM was about 380 GM [29] in DCM. They were both higher than BM-PPPM-C6. This may be because the fluorescence quantum yield of BD-PPM (52.1%) was much higher than that of BD-PPM (16.0% in DCM) and BD-PTM (40.3% in DCM), resulting in a smaller calculated value of δ_{TPA}.

4.3. Cyclic Voltammograms

Cyclic voltammetry can be put to proper use by approximating the orbital energy levels of molecules. The experiment was carried out in a DCM solution of 0.1 mol/L of n-Bu$_4$NPF$_6$. In the experiment, a platinum sheet was employed as the working electrode, platinum wire was used as the counter electrode, an Ag/Ag$^+$ electrode was used as the reference electrode, and ferrocene was used as the internal standard. The scan rate was set to 0.1 V/s. It can be calculated from Figure 5 that $E_{\text{HOMO}} = -5.26$ eV. Taking into account the approximate conditions used in the theoretical calculations, it can be considered that the experimental results are basically in line with the theoretical ones. From the ultraviolet–visible absorption band edge of the molecule, the optical band gap of the molecule is around 446 nm, $E_g = 2.78$ eV. If the optical band gap of the molecule is approximately regarded as the molecular energy gap, the calculation can be $E_{\text{LUMO}} = -2.48$ eV.
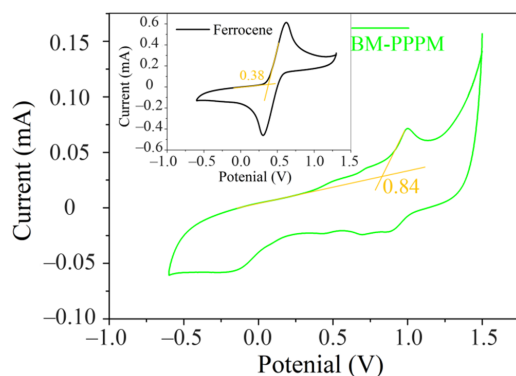

Figure 5. Cyclic voltammetry experiments of molecule BM-PPPM-C6 and ferrocene at a concentration of 1×10^{-3} mol/L in DCM.

4.4. UV Light Stability

Under the ultraviolet light, the photolysis properties of molecules can indicate the sensitivity of molecules to ultraviolet light. Molecules with a concentration of 1×10^{-5} mol/L are irradiated by ultraviolet light with a wavelength of 365 nm and a light intensity of 50 mW/cm^2 in a DCM solution. The data of the photolysis experiment are shown in Figure 6a. It can be seen that the molecules react easily under ultraviolet irradiation, indicating that they have high photosensitivity, which also means that the molecule needed to be kept away from light during use.

As shown in Figure 6b, the early photolysis process of the molecule conforms to the first-order kinetic model, and its concentration decays exponentially with time by fitting the relationship between the absorbance of the molecule at 394 nm and the irradiation

time. This has a certain value for studying the principle and kinetic process of molecular initiation polymerization.
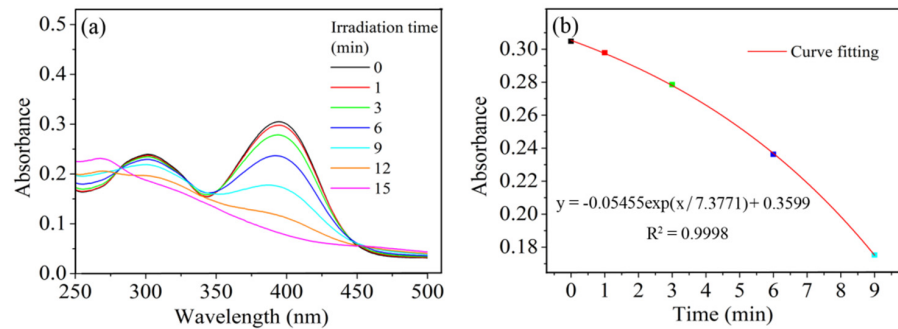
Figure 6. (**a**) UV degradation characteristics of molecule BM-PPPM-C6 at a concentration of 1×10^{-5} mol/L. (**b**) Photodegradation versus time fitting curve.

4.5. TPPAM Experiments

After analyzing the optical properties of the molecule, it is confirmed that the molecule has potential as an initiator. However, the actual initiation performance needs to be tested in a two-photon polymerization experiment. The experiment of TPPAM was carried out with the molecule BM-PPPM-C6 as the initiator and TMPTA as the monomer. In Figure 7a, it is shown that the molecule can actually initiate the polymerization of the monomer to form a three-dimensional structure. At a lower writing speed of 100 µm/s, polymerization is still able to initiate when the power is as low as 5 mW. Under an extremely high writing speed of 100,000 µm/s, the power of 30–50 mW is able to initiate polymerization to form a complete three-dimensional structure. Figure 7b,c is the enlarged structure of the area shown. As can be seen, the molecule can be used as an initiator to obtain a three-dimensional structure with clear outline and complete structure under the applicable speed and power conditions, which proves that the molecule BM-PPPM-C6 is successful as an initiator.
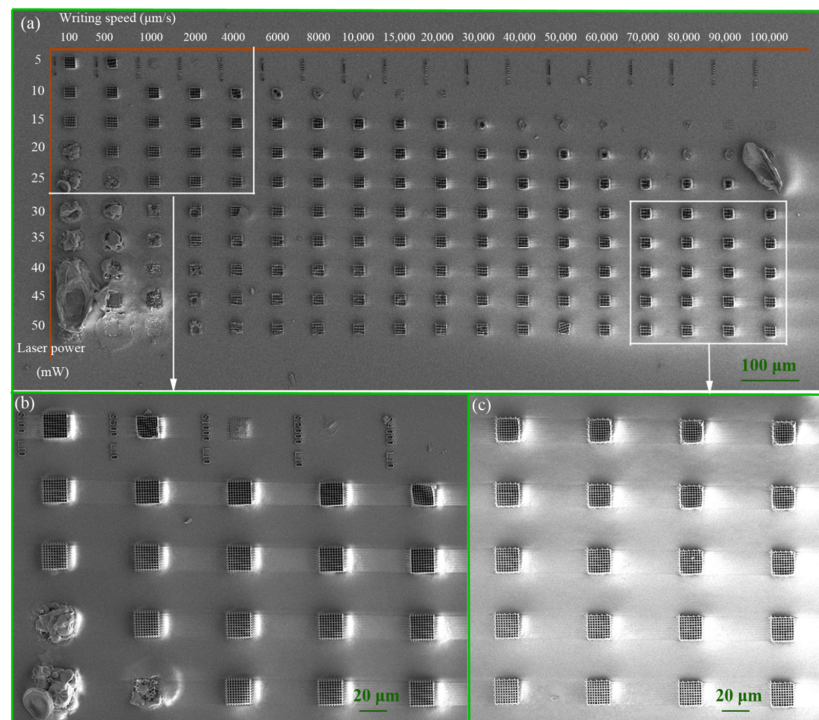
Figure 7. (**a**) SEM images of structures with initiator BM-PPPM-C6 (10 µmol/g) in TMPTA. (**b**) Enlarged view of low writing speed area. (**c**) Enlarged view of high writing speed area.

The designed BM-PPPM series of molecules are equipped with different alkane chain lengths. Although it is generally believed that the chain length of alkane hardly affects the chemical properties of the molecule, the solubility of the molecule and the interaction between the molecule and the monomer will have a certain difference in reality. It is not known whether these differences may have a certain impact on the initiation efficiency of the molecule. Consequently, the polymerization effect of BM-PPPM with different alkane chain lengths in TMPTA was compared, as shown in Figures 8 and S5–S7. It can be seen that under the same initiator concentration, there is no obvious difference in the initiation effect of the designed molecule in TMPTA. Initiator molecules of different chain lengths can be completely dissolved in TMPTA to achieve polymerization.
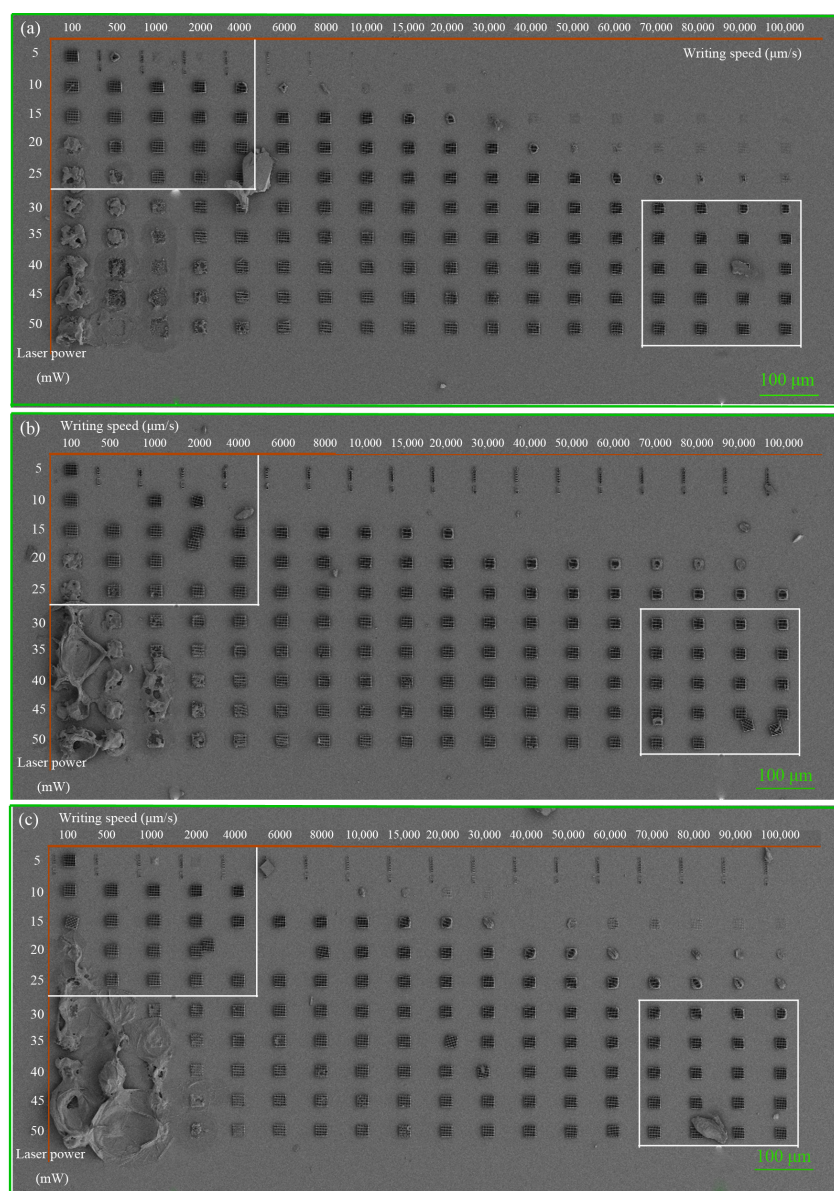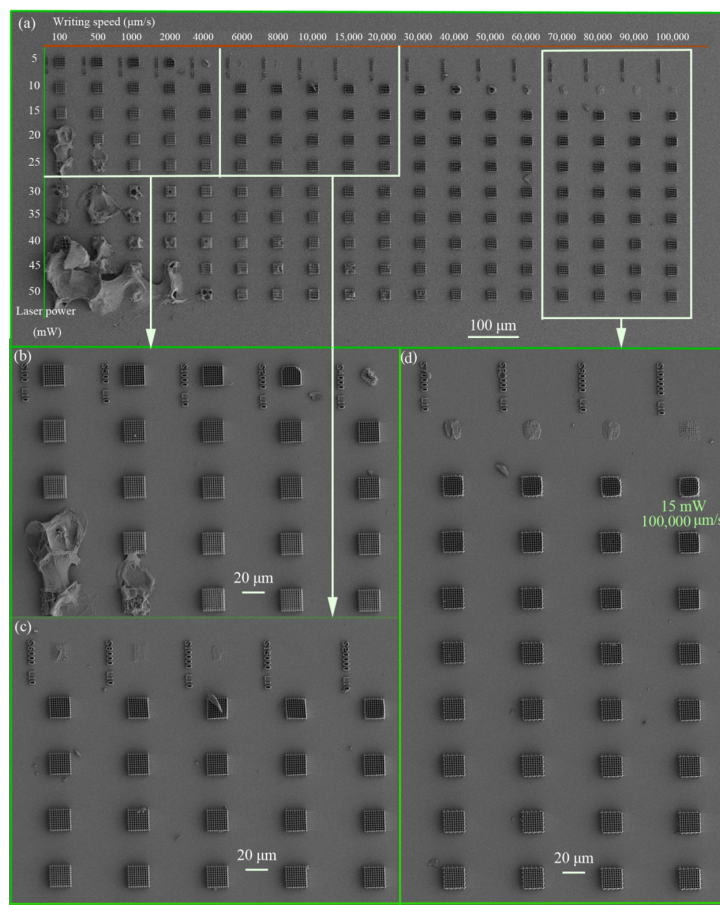

Figure 8. SEM images of structures with initiators (**a**) BM-PPPM-C12; (**b**) BM-PPPM-C16; and (**c**) BM-PPPM-C20 in TMPTA, 10 μmol/g.

BM-PPPM is obtained by conjugation expansion, so the changes in the initiating ability of molecules with diverse degrees of conjugation are interesting. Comparing the initiation efficiency of BM-PPPM with BD-PPM and BD-PM in previous work [28,29], it can be found that the initiation efficiency of BM-PPPM has been greatly improved compared to BD-PPM

and BD-PM, which is in line with the expected improvement in initiator efficiency due to conjugation extension.

However, when BM-PPPM was compared to a more highly conjugated triphenylamine molecule (BM-PTM) [29], it was found that its initiation effect was not inferior; this indicates that simply adding a conjugation group gradually lessened the increase in initiation efficiency as the degree of conjugation increased, just like the diminishing marginal utility effect. Hence, it should not be achieved simply by conjugation expansion, but requires more in-depth consideration so as to design a larger and more efficient initiator.

Although molecules with diverse alkane chain lengths have complete solubility in TMPTA, it does not mean that the molecules with different chain lengths are meaningless. When using the monomer PETA, it was found that hardly any of the BM-PPPM-C6 can be completely dissolved. Additionally, the molecules with longer carbon chains cannot form a clear and transparent dissolution in PETA. After two days of heating and stirring, precipitation still exists. This shows that for PETA, the molecule BM-PPPM-C6 alone can be used as a suitable initiator. As shown in Figure 9, it is more effective in initiating polymerization in PETA, BM-PPPM-C6. With a power of 15 mW and a speed of up to 100,000 μm/s, it can still form a complete three-dimensional structure with only slight deformation at the edges. This result is better than the test results under the same conditions reported in the recent literature (when the writing speed was 100,000 μm/s, the minimum laser power was 44 mW) [15]. Under low speed, low power and a power condition of 5 mW, polymerization can be realized in the speed range of 100–2000 μm/s, with a larger range of polymerization parameters. The above results are excellent, which suggests that this molecule can be used in additive manufacturing at high speeds. Compared to the molecules formed by benzophenone and triphenylamine, the test results in PETA are not inferior.

Figure 9. (**a**) SEM images of structures with initiators BM-PPPM-C6 in PETA, 10 μmol/g. (**b**–**d**) Enlarged images of the area shown.

Meanwhile, in order to illustrate that initiators with different alkane chain lengths have different compatibility in some monomers, the solubility of BM-PPPM series molecules was studied using n-heptane as a solvent. It was found that BM-PPPM-C6 and BM-PPPM-C16 had poor solubility; conversely, BM-PPPM-C20 had good solubility, as shown in Figure S8. BM-PPPM-C12 will separate out after standing for a period of time. At this solvent polarity, longer-chain alkanes are more favorable for dissolution. This entirely illustrates that controlling the alkane chain can effectively regulate the solubility of molecules with different solvents, ensuring that only the change in the alkane chain can meet the needs of different monomers for initiators.

In consequence, it can be seen that due to the critical factor of solubility, the length of the alkane chain is not meaningless in the process of being an initiator. The solubility between organics is extremely complicated, and it is tough to accurately determine the degree of solubility. The simple act of introducing carbon chains of different lengths can effectively change the solubility of molecules. However, in the monomer PETA selected in this article, the shortest chain is more conducive to dissolution. Nevertheless, longer alkane chains may have better solubility under certain conditions. Furthermore, only an alkane chain of moderate length can dissolve more effectively.

5. Conclusions

In this paper, a BM-PPPM series of D–π–A–π–D molecules based on benzophenone groups were designed by conjugated extension. Through theoretical calculations and photophysical experiments, the potential of molecules as nonlinear materials was confirmed. Through TPPAM experiments, it is proven that PETA resin with BM-PPPM molecules as initiators can form complete three-dimensional structures at a writing speed as high as 100,000 μm/s and a laser power as low as 15 mW.

From a molecular-structure point of view, it is confirmed that the molecular conjugate extension can indeed improve molecular initiation efficiency. However, as the degree of conjugation reaches a certain limit, the improvement that can be brought by adding conjugated groups will be extremely limited. In addition, the chain length of the initiator will obviously affect the solubility with the monomer. By simply changing the alkane chain length, the compatibility relationship between the initiator and the monomer can be enhanced to a certain extent.

Data Availability Statement: Some or all of the data, models, or code generated or used during the study are available from the corresponding author by request.

Conflicts of Interest: There are no conflict of interest to declare.

References

1. Sun, H.; Mizeikis, V.; Xu, Y.; Juodkazis, S.; Ye, J.; Matsuo, S.; Misawa, H. Microcavities in polymeric photonic crystals. *Appl. Phys. Lett.* **2001**, *79*, 1–3. [CrossRef]
2. Serbin, J.; Egbert, A.; Ostendorf, A.; Chichkov, B.N.; Houbertz, R.; Domann, G.; Schulz, J.; Cronauer, C.; Fröhlich, L.; Popall, M. Femtosecond laser-induced two-photon polymerization of inorganic-organic hybrid materials for applications in photonics. *Opt. Lett.* **2003**, *28*, 301–303. [CrossRef] [PubMed]
3. Morales-Delgado, E.E.; Urio, L.; Conkey, D.B.; Stasio, N.; Moser, D.P.C. Three-dimensional microfabrication through a multimode optical fiber. *Opt. Express.* **2016**, *25*, 7031–7045. [CrossRef] [PubMed]
4. Gissibl, T.; Thiele, S.; Herkommer, A.; Giessen, H. Two-photon direct laser writing of ultracompact multi-lens objectives. *Nat. Photonics* **2016**, *10*, 554–560. [CrossRef]
5. Cumpston, B.H.; Ananthavel, S.P.; Barlow, S.; Dyer, D.L.; Ehrlich, J.E.; Erskine, L.L.; Heikal, A.A.; Kuebler, S.M.; Lee, I.-Y.S.; Maughon, D.; et al. Two-photon polymerization initiators for three-dimensional optical data storage and microfabrication. *Nature* **1999**, *398*, 51–54. [CrossRef]
6. Parthenopoulos, D.A.; Rentzepis, P.M. Three-dimensional optical storage memory. *Science* **1989**, *245*, 843–845. [CrossRef]
7. Yuan, X.; Zhao, M.; Guo, X.; Gan, Z.; Ruan, H. Ultra-high capacity for three-dimensional optical data storage inside transparent fluorescent tape. *Opt. Lett.* **2020**, *45*, 1535–1538. [CrossRef]
8. Moussi, K.; Bukhamsin, A.; Hidalgo, T.; Kosel, J. Biocompatible 3D Printed Microneedles for Transdermal, Intradermal, and Percutaneous Applications. *Adv. Eng. Mater.* **2020**, *22*, 1901358. [CrossRef]
9. Balčiūnas, E.; Baldock, S.J.; Dreižė, N.; Grubliauskaitė, M.; Coultas, S.; Rochester, D.L.; Valius, M.; Hardy, J.G.; Baltriukienė, D. 3D printing hybrid organometallic polymer-based biomaterials via laser two-photon polymerization. *Polym. Int.* **2019**, *68*, 1928–1940. [CrossRef]
10. Wu, D.; Wu, S.Z.; Xu, J.; Niu, L.G.; Midorikawa, K.; Sugioka, K. Hybrid femtosecond laser microfabrication to achieve true 3D glass/polymer composite biochips with multiscale features and high performance: The concept of ship-in-a-bottle biochip. *Laser Photonics Rev.* **2014**, *8*, 458–467. [CrossRef]
11. Zhou, X.; Hou, Y.; Lin, J. A review on the processing accuracy of two-photon polymerization. *AIP Adv.* **2015**, *5*, 030701. [CrossRef]
12. Nazir, R.; Thorsted, B.; Balčiūnas, E.; Mazur, L.; Deperasińska, I.; Samoć, M.; Brewer, J.; Farsari, M.; Gryko, D.T. π-Expanded 1, 3-diketones–synthesis, optical properties and application in two-photon polymerization. *J. Mater. Chem. C* **2016**, *4*, 167–177. [CrossRef]
13. Malval, J.-P.; Jin, M.; Morlet-Savary, F.; Chaumeil, H.; Defoin, A.; Soppera, O.; Scheul, T.; Bouriau, M.; Baldeck, P.L. Enhancement of the two-photon initiating efficiency of a thioxanthone derivative through a chevron-shaped architecture. *Chem. Mater.* **2011**, *23*, 3411–3420. [CrossRef]
14. Jia, X.; Zhao, D.; You, J.; Hao, T.; Li, X.; Nie, J.; Wang, T. Acetylene bridged D-(π-A)2 type dyes containing benzophenone moieties: Photophysical properties, and the potential application as photoinitiators. *Dyes Pigments* **2021**, *184*, 108583. [CrossRef]
15. Zhang, F.; Hu, Q.; Castañon, A.; He, Y.; Liu, Y.; Paul, B.T.; Tuck, C.J.; Hague, R.J.M.; Wildman, R.D. Multi-branched benzylidene ketone based photoinitiators for multiphoton fabrication. *Addit. Manuf.* **2017**, *16*, 206–212. [CrossRef]
16. Hao, F.; Liu, Z.; Zhang, M.; Liu, J.; Zhang, S.; Wu, J.; Zhou, H.; Tian, Y.P. Four new two-photon polymerization initiators with varying donor and conjugated bridge: Synthesis and two-photon activity. *Spectrochim. Acta Part A* **2014**, *118*, 538–542. [CrossRef]
17. Li, Z.; Rosspeintner, A.; Hu, P.; Zhu, G.; Hu, Y.; Xiong, X.; Peng, R.; Wang, M.; Liu, X.; Liu, R. Silyl-based initiators for two-photon polymerization: From facile synthesis to quantitative structure–activity relationship analysis. *Polym. Chem.* **2017**, *8*, 6644–6653. [CrossRef]
18. Jin, M.; Hong, H.; Xie, J.C.; Malval, J.P.; Spangenberg, A.; Soppera, O.; Wan, D.C.; Pu, H.T.; Versace, D.L.; Leclerc, T.; et al. π-conjugated sulfonium-based photoacid generators: An integrated molecular approach for efficient one and two-photon polymerization. *Polym. Chem.* **2014**, *5*, 4747–4755. [CrossRef]
19. Li, S.; Lu, C.; Wan, X.; Zhang, S.; Li, J.; He, Z.; Zhang, L. Enhancement of two-photon initiation efficiency based on conjugated phenothiazine and carbazole derivatives. *Mater. Today Commun.* **2020**, *24*, 101219. [CrossRef]
20. Li, S.; Hu, J.; Zhang, S.; Feng, C.; Zhang, L.; Wang, C.; He, Z.; Zhang, L. Novel A-π-D-π-A structure two-photon polymerization initiators based on phenothiazine and carbazole derivatives. *Chem. Pap.* **2021**, *75*, 5249–5256. [CrossRef]
21. Nazir, R.; Bourquard, F.; Balciunas, E.; Smolen, S.; Gray, D.; Tkachenko, N.V.; Farsari, M.; Gryko, D.T. π-Expanded α, β-Unsaturated Ketones: Synthesis, Optical Properties, and Two-Photon-Induced Polymerization. *ChemPhysChem* **2015**, *16*, 682–690. [CrossRef] [PubMed]
22. Fang, H.; Gao, H.; Wang, T.; Zhang, B.; Xing, W.; Cheng, X. Benzothiadiazole-based D-π-A-π-D fluorophores: Synthesis, self-assembly, thermal and photophysical characterization. *Dyes Pigments* **2017**, *147*, 190–198. [CrossRef]

23. Nazir, R.; Balčiunas, E.; Buczyńska, D.; Bourquard, F.; Kowalska, D.; Gray, D.; Maćkowski, S.; Farsari, M.; Gryko, D.T. Donor–Acceptor Type Thioxanthones: Synthesis, Optical Properties, and Two-Photon Induced Polymerization. *Macromolecules* **2015**, *48*, 2466–2472. [CrossRef]

24. Hu, P.; Zhu, J.; Liu, R.; Li, Z. Conjugated Ketocarbazoles as Efficient Photoinitiators: From Facile Synthesis to Efficient Two-photon Polymerization. *Photopolym. Sci. Technol.* **2019**, *32*, 257–264. [CrossRef]

25. Jia, X.; Han, W.; Xue, T.; Zhao, D.; Li, X.; Nie, J.; Wang, T. Diphenyl sulfone-based A–π-D–π-A dyes as efficient initiators for one-photon and two-photon initiated polymerization. *Polym. Chem.* **2019**, *10*, 2152–2161. [CrossRef]

26. Zheng, Y.-C.; Zhao, Y.-Y.; Zheng, M.-L.; Chen, S.-L.; Liu, J.; Jin, F.; Dong, X.-Z.; Zhao, Z.-S.; Duan, X.-M. Cucurbit[7]uril-Carbazole Two-Photon Photoinitiators for the Fabrication of Biocompatible Three-Dimensional Hydrogel Scaffolds by Laser Direct Writing in Aqueous Solutions. *ACS Appl. Mater. Interfaces* **2019**, *11*, 1782–1789. [CrossRef] [PubMed]

27. Huang, X.; Wang, X.; Zhao, Y. Study on a series of water-soluble photoinitiators for fabrication of 3D hydrogels by two-photon polymerization. *Dyes Pigments* **2017**, *141*, 413–419. [CrossRef]

28. Li, Z.; Siklos, M.; Pucher, N.; Cicha, K.; Ajami, A.; Husinsky, W.; Rosspeintner, A.; Vauthey, E.; Gescheidt, G.; Stampfl, J.; et al. Synthesis and structure-activity relationship of several aromatic ketone-based two-photon initiators. *J. Polym. Sci. Part A Polym. Chem.* **2011**, *49*, 3688–3699. [CrossRef]

29. Zhang, S.; Li, S.; Wan, X.; Ma, J.; Li, N.; Li, J.; Yin, Q. Ultrafast, high-resolution and large-size three-dimensional structure manufacturing through high-efficiency two-photon polymerization initiators. *Addit. Manuf.* **2021**, *47*, 102358. [CrossRef]

30. Gan, X.; Wang, Y.; Ge, X.; Li, W.; Zhang, X.; Zhu, W.; Zhou, H.; Wu, J.; Tian, Y. Triphenylamine isophorone derivatives with two photon absorption: Photo-physical property, DFT study and bio-imaging. *Dyes Pigments* **2015**, *120*, 65–73. [CrossRef]

31. Silva, D.L.; de Boni, L.; Correa, D.S.; Costa, S.C.S.; Hidalgo, A.A.; Zilio, S.C.; Canuto, S.; Mendonca, C.R. Two-photon absorption in oxazole derivatives: An experimental and quantum chemical study. *Opt. Mater.* **2012**, *34*, 1013–1018. [CrossRef]

32. Frisch, M.J.; Trucks, G.W.; Schlegel, H.B.; Scuseria, G.E.; Robb, M.A.; Cheeseman, J.R.; Scalmani, G.; Barone, V.; Mennucci, B.; Petersson, G.A.; et al. *Gaussian 09, Revision D.01*; Gaussian, Inc.: Wallingford, CT, USA, 2013.

33. Santos, B.; Gonçalves, A.; Souza, A.; Freitas, C.; Cabral, L.; Albuquerque, M.; Castro, H.; Santos, E.; Rodrigues, C. Molecular Modeling Studies of the Structural, Electronic, and UV Absorption Properties of Benzophenone Derivatives. *J. Phys. Chem. A* **2012**, *116*, 10927–10933. [CrossRef]

34. Sonogashira, K.; Tohda, Y.; Hagihara, N. A Convenient Synthesis of Acetylenes: Catalytic Substitutions of Acetylenic Hydrogen with Bromoalkenes, Iodoarenes and Bromopyridines. *Tetrahedron Lett.* **1975**, *16*, 4467–4470. [CrossRef]

35. Xu, C.; Webb, W.W. Measurement of two-photon excitation cross sections of molecular fluorophores with data from 690 to 1050 nm. *J. Opt. Soc. Am. B* **1996**, *13*, 481–491. [CrossRef]

36. Haq, B.S.; Khan, H.U.; Alam, K.; Ajmal, M.; Attaullah, S.; Zari, I. Determination of two-photon absorption cross sections of photosensitizers and its implications for two-photon polymerization. *Appl. Opt.* **2015**, *54*, 132–140. [CrossRef]